Periodically arranged colloidal gold nanoparticles for enhanced light harvesting in organic solar cells

Mina Mirsafaei[1,a)], André Luis Fernandes Cauduro[1], Casper Kunstmann-Olsen[2], Adam Michael Davidson[2], Søren Hassing[3],Martin A.B. Hedegaard[3] ,Horst-Günter Rubahn[1], Jost Adam[1], and Morten Madsen[1]

[1]SDU NanoSYD, Mads Clausen Institute, University of Southern Denmark, Alsion 2, Sønderborg, DK-6400, Denmark; [2]Dept. of Chemistry, University of Liverpool, Crown Street, L69 7ZD, Liverpool,United Kingdom; [3]Department of Chemical Engineering, Biotechnology and Environmental Technology, University of Southern Denmark, Campusvej 55, 5230 Odense M, Denmark

ABSTRACT

Although organic solar cells show intriguing features such as low-cost, mechanical flexibility and light weight, their efficiency is still low compared to their inorganic counterparts. One way of improving their efficiency is by the use of light-trapping mechanisms from nano- or microstructures, which makes it possible to improve the light absorption and charge extraction in the device's active layer. Here, periodically arranged colloidal gold nanoparticles are demonstrated experimentally and theoretically to improve light absorption and thus enhance the efficiency of organic solar cells. Surface-ordered gold nanoparticle arrangements are integrated at the bottom electrode of organic solar cells. The resulting optical interference and absorption effects are numerically investigated in bulk hetero-junction solar cells based on the Finite-Difference Time-Domain (FDTD) and Transfer Matrix Method (TMM) and as a function of size and periodicity of the plasmonic arrangements. In addition, light absorption enhancement in the organic active layer is investigated experimentally following integration of the nanoparticle arrangements. The latter are fabricated using a lithography-free stamping technique, creating a centimeter scaled area with nanoparticles having a defined inter-particle spacing. Our study reveals the light harvesting ability of template-assisted nanoparticle assemblies in organic solar cells. As the approach is easily scalable, it is an efficient and transferable method for large-scale, low cost device fabrication.

Keywords: Plasmonic nanoparticles, organic semiconductors, organic solar cells, light-trapping, soft nano-imprint lithography, gold nanoparticles

1. INTRODUCTION

The photovoltaic (PV) market is currently dominated by silicon solar cells, mainly due to their high power conversion efficiencies. They are, however, material intensive, which has led to the development of solar cells based on organic semiconductors. The ease of processing organic materials, the low material and fabrication costs along with the possibility of making ultra-thin and flexible devices render organic solar cells ideal candidates for the future renewable energy market. Over the past ten years, investigations on the synthesis of new organic semiconductors, on morphological optimizations and on new device structures have led to improved organic solar cell performances. Nevertheless, organic solar cells still show relatively low power conversion efficiencies, mainly due to inherent drawbacks such as short exciton diffusion lengths [1] and low carrier mobilities. The resulting loss mechanisms lead to hampered device performances, especially for optically thick devices.

[a)] Electronic mail: mirsafaei@mci.sdu.dk

One of the approaches to improve the device performance is by increasing the light absorption in the active layer, for example by using nano- or microstructures that diffract light at specific wavelengths into large angles in the active layers [2-4], or by utilizing the Localized Surface Plasmon Resonance (LSPR) effect of metal nanoparticles (MNPs) [5]. The use of such light trapping mechanisms also makes it possible to improve charge extraction, as it allows for the fabrication of thinner devices without compromising light absorption. In particular, use of metal nanoparticles made from gold and silver has received significant attention for use in organic solar cell applications, due to effective plasmonic effects. The introduction of metallic nanoparticles directly into the active layer [6-8] or the incorporation of plasmonic metal nanoparticles in the electron and hole transport layer [7, 9-15] has been studied in order to enhance the performance of organic solar cells. Novel metal nanostructures and their alloys have been the subject of extended studies owing to their plasmonic behavior, including their ability to support Surface Plasmon Polaritons (SPPs) aside from LSPRs. The optical effects of the nanoparticles are tunable and depend on parameters defined by the nature of their building blocks and the assembly structure such as shape, size, inter-particle distance and colloidal distribution [8, 16]. However, the narrow resonant wavelength region for metallic nanostructures is typically limiting the ability to obtain strong efficiency enhancements from this approach. In addition, as the particle location within the solar cell is crucial for the optical performance, random arrangements and uncontrolled aggregation of NPs may cause undesirable exciton quenching and also short-circuits within the device [11]. Theoretical investigations from, e.g., Finite-Difference Time-Domain (FDTD) studies can be employed to study these optical effects in detail, and thus also to assist in deciding on the most promising design rules for device fabrication, in order to maximize the effect from MNPs in organic solar cells.

In this paper, we investigate experimentally the light absorption enhancement in the organic active layer by incorporating surface-ordered gold nanoparticle arrangements at the bottom electrode in organic solar cells (see the experimental section). We experimentally demonstrate absorption enhancements in the cells originating from the implemented Ag metallic nanogratings and Au nanoparticles. In addition, we provide theoretical studies to clarify and understand the physical origins of light absorption enhancement in the presented devices. More specifically, we study the optical interference and absorption in multilayer organic solar cell stacks via numerical analyses based on FDTD and TMM. Based on our FDTD model, we investigate the influence of parameters such as the period and the size of the periodic nanoparticle arrangements in the organic solar cells.

This article is structured as follows: Section 2 briefly explains the fabrication method of the organic solar cells with integrated, periodically arranged nanoparticles. Section 3 explains the numerical methods, which are used in order to calculate the absorption within the device. Section 4 discusses the optical effects that are induced by incorporation of the dual metallic nanostructures within the organic solar cell. Section 5 concludes our results.

2. EXPERIMENTAL SECTION

We demonstrate the integration of dual metallic nanostructures composed of Au NPs (i.e., for LPR) at the interface between the poly-3-hexylthiophene:[6,6]-phenyl-C 61 -butyric acid methyl ester (P3HT:$PC_{60}BM$) active layer and the hole transport layer (HTL), followed by the formation of the silver (Ag) grating electrode as the back reflector in inverted OSCs. Figure 1 describes the fabrication method of the periodically arranged Au nanoparticles in organic solar cells. First, we fabricate the inverted organic solar cell with the device structure of Indium Thin Oxide (ITO) covered by an alcohol-/water-soluble conjugated polymer, poly [(9,9-bis(3′-(N,N-dimethylamino)propyl)-2,7-fluorene)-alt-2,7-(9,9–dioctylfluorene)] (PFN) [17], and a blend of P3HT:$PC_{60}BM$ (1:1 weight ratio) as a photoactive layer, where the thicknesses of PFN and active layer are 10 nm and 200 nm, respectively. Then, in order to introduce the periodically arranged metallic nanoparticles, we propose to use a

soft nano-imprint method to directly pattern and transfer the nanoparticles on the active layer, using a wrinkled PDMS template (see method section). By evaporating the 10 nm of MoO_x and 100 nm of silver on the periodically arranged nanoparticles, the anode follows the surface profile of the active layer, and thus the grating features are present on the Ag electrode.

To explain the light trapping nature of the integrated nanoparticles in the cells, and in order to distinguish between the effect of the grating structure and the periodically arranged Au NPs, we extracted the absorption from diffuse reflection (R) and diffuse transmission (T), analyzing 1-R-T for a planar solar cell and a solar cell with integrated grating structure and periodically arranged nanoparticles, respectively. Moreover, we used scanning electron microscopy to evaluate the assembly process on the PDMS samples and the imprint process in order to investigate the coverage over larger areas.

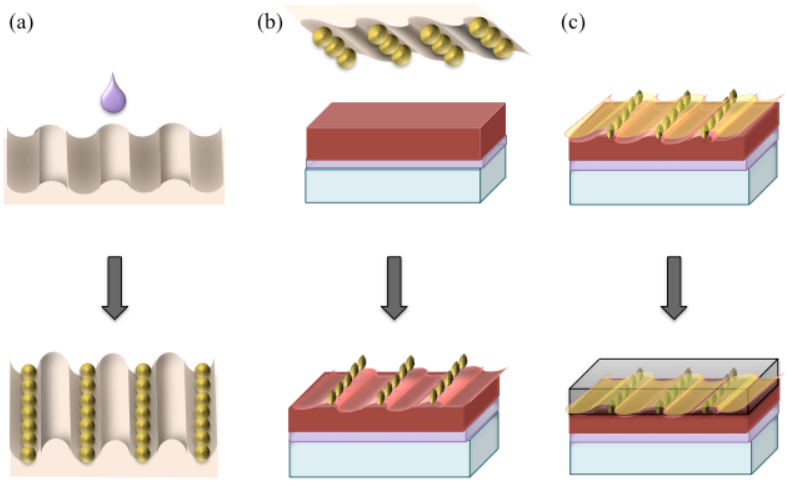

Figure 1. Schematic of organic solar cell fabrication: a) Drop casting of the highly concentrated polyethylene glycol (PEG)-capped Au nanoparticles on wrinkled poly (dimethylsiloxane) (PDMS) template, b) soft imprint of nanoparticles on active layer, applying a 500g weight on the backside of the PDMS templates, pressing it against the ITO substrate coated with PFN and active layer and c) periodically arranged Au nanoparticle on active layer followed by thermal evaporation of MoOx and Ag.

3. NUMERICAL METHODS

The optical absorption of a solar cell can be calculated via the FDTD method, which makes it possible to determine the spatial distribution of the electromagnetic field versus time and position, and thus, the generation rate inside the organic solar cell (OSC). In this work, the calculation was carried out using the FDTD software implementation from Lumerical. The materials' complex refractive indices were taken from literature [17-21]. The results of the FDTD model were compared with numerical analysis from the transfer matrix method, which calculates the reflection and transmission at each interface as well as the attenuation in each layer [22-25].

In our FDTD model, the periodic boundary conditions are implemented for *x* and *y* directions and perfectly matched layer (PML) boundary conditions are used for *z* direction. A normally incident plane wave polarized along the x-axis is used as a source of illumination. The space mesh size lower that 2 nm has been chosen depending on the NPs dimension. The device structure and detailed parameters are shown in Figure 2 and Table 1.

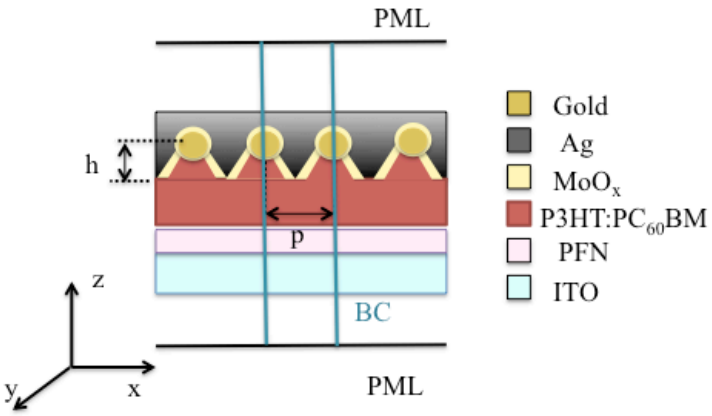

Figure 2. Cross section view of 2-D schematic design used for the FDTD calculation, showing the perfectly matched layer (PML) boundary conditions, which is used for the up and down z direction, and the periodic boundary condition (BC) is used for x direction. The height of grating structure (h) has been set to 70 nm and P shows the period of the grating structure (300 nm, 500 nm and 700 nm).

Table 1. Material thicknesses of the solar cell

Material	Thickness (nm)
Silver	100
MoO_3	10
P3HT: $PC_{60}BM$	200
PFN	10
ITO	150

4. RESULTS AND DISCUSSIONS

We study the optical effect from the periodically arranged nanoparticles integrated on the organic solar cell having a 15 nm nanoparticle size and a period of 684 nm. We experimentally demonstrate a broadband absorption enhancement, which can be explained by the strong near field caused from LPR of Au NPs embedded at the interface of the active layer and HTL together with the diffraction effect of the grating structure. The results from the diffuse reflection and transmission spectra

are demonstrated in Figure 3. Scanning Electron Microscopy (SEM) images of the periodical arrangement of Au NPs on active layer is shown in Figure 4.

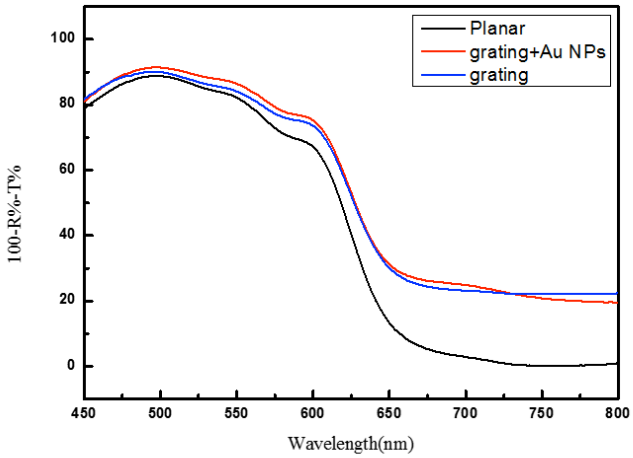

Figure 3. Absorption (100-R%-T%) spectrum of the ITO/PFN/P3HT: $PC_{60}BM$/MoOx/Ag solar cell showing the planar structure (black line), the grating imprinted structure (blue line) and the grating with periodically arranged Au NPs on active layer, i.e. containing both NPs and the grating structure (red line).

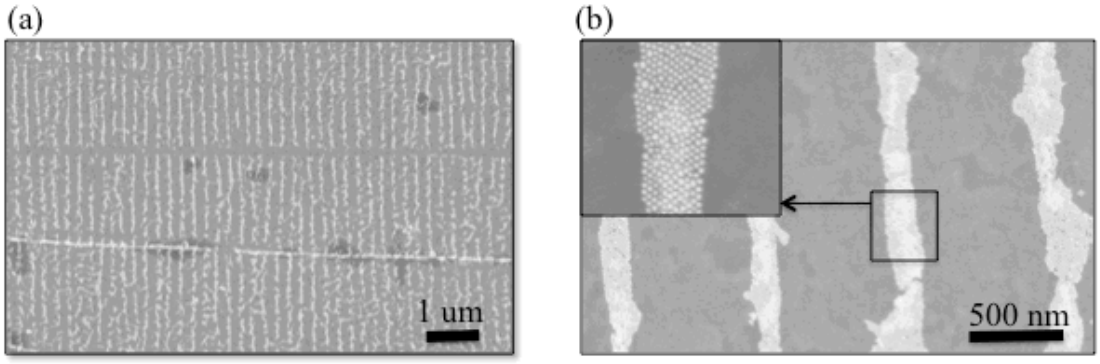

Figure 4. Scanning electron microscope (SEM) images of the periodically self-assembly of gold nanoparticles on active layer showing on a) assembly process over a large area, and b) individual Au NP chains in detail. In the inset, it is shown that each chain has approximately eleven Au NPs (diameter of 15 nm) with a relatively homogeneous surface coverage over a large area.

Compared to the reference OSCs without NPs or grating structures, the diffuse reflection of the OSC containing the grating structure decreases, indicating that more light is absorbed in this device. In addition, by incorporating the periodical Au nanoparticles in the OSC, the diffuse reflection drops further, which can be explained by the nanoparticle LSPR, leading to an increased absorption enhancement in the cells. Experimentally, we find that the Ag grating structure has a greater impact on absorption at a wavelength region above approx. 550 nm, whereas the Au nanoparticles mainly offer improved light absorption enhancement in the wavelength range from 450 nm to 600 nm, compared to the grating structure.

Following our experimental results, to clarify the physical origins of the light absorption enhancement in the devices, we solve Maxwell's equations by using the FDTD method. Figure 5 shows the absorption spectrum of the solar cell with the configuration of Ag/MoO_x/P3HT: PCBM/PFN/ITO calculated by both the FDTD and TMM method. The absorption calculated by the FDTD model and the TMM for these planar OSCs are in a good agreement.

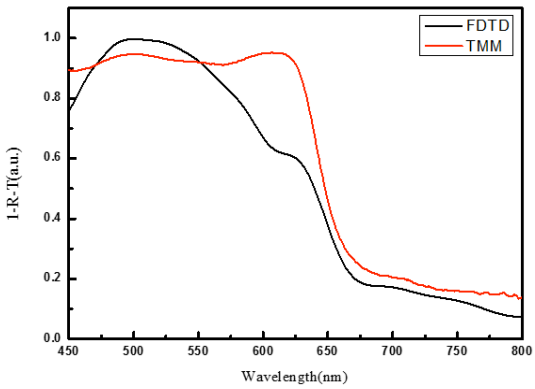

Figure 5.Absorption of a planar organic solar cell calculated with FDTD method and TMM.

Based on our model, we demonstrate the effect from integration of the dual metallic nanostructures, which is composed of periodically arranged colloidal gold (Au) nanoparticles embedded at the interface between the active layer and hole transport layer (HTL) leading also to a grating patterned Ag electrode. In order to understand the optical effect due to the grating structure and the gold nanoparticles separately, we first studied light harvesting in the active layer with one type of metallic nanostructure, the Ag grating electrode. Then, we investigated the effect from the periodical arrangement of Au NPs in the organic solar cell. Figure 6 shows the optical absorption enhancement in the device originating from the Ag grating structure alone and from the dual metallic nanostructure, the combined Ag grating and chain of Au nanoparticles, having the same period as for the grating structure (particle size is 15 nm in diameter) .The interparticle gap between the particles inside of the chain has been chosen to be 2 nm.

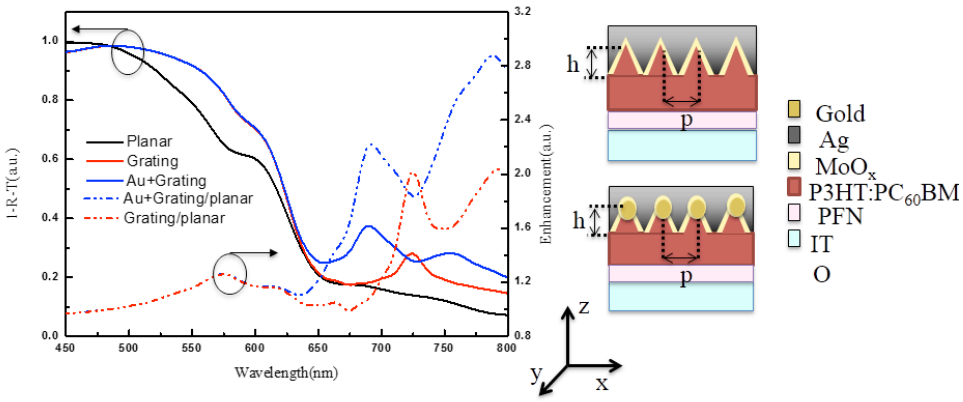

Figure 6. FDTD-calculated device absorption (1-reflection-transmission) and the absorption enhancement for a planar reference OSC, as compared to an OSC with grating structure and to a device with periodically arranged Au NPs. The grating structure and periodically arranged nanoparticles show a broadband absorption enhancement in the wavelength range of 500 nm to 800 nm compared to planar solar cell. In addition, by adding the Au NPs on the grating structure, the absorption enhancement is increased further in the range of 650 nm to 800 nm.

The absorption spectrum of the device with the grating structure and grating structure plus chain of nanoparticles shows broadband enhancement compared to the planar organic solar cell. The Ag grating structure shows light absorption enhancement in the wavelength range of 500 nm to 800 nm for the period of 700 nm [26]. After incorporation of the periodically arranged Au nanoparticles together with the grating structure, we observe a stronger optical enhancement in the frequency range of 600 nm to 800 nm. A peak centered around 700 nm shows up in our simulation model, however, does not appear in the experimental measurement shown in Figure 3. This is probably due to the use of non-polarized light illumination in our experimental setup. For our simulation model, on the other hand, we have used TM polarized light source, which can be interpreted as a coupling phenomena of LPR with the Floquet mode of the Ag grating structures (see electric field intensity profile in figure 9). The electric field intensity of the organic solar cell with a grating structure and periodically arranged nanoparticles is shown in Figure 6. According to the electric field intensity ($|E|^2$) calculated within the device at a wavelength of 600 nm, the near field enhancement lies mostly near the MoOx layer, and therefore light scattering is the main effect responsible for the enhanced absorption at this wavelength [27].

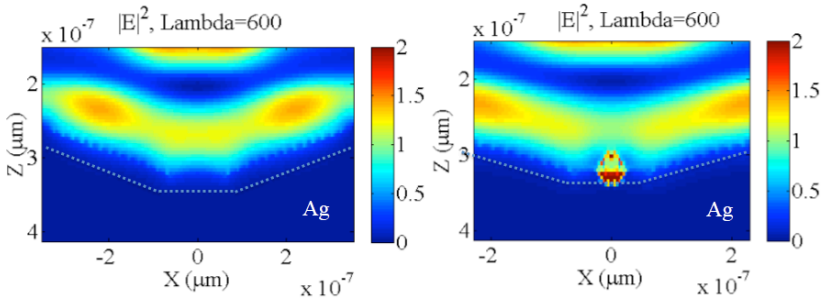

Figure 6. Electric field intensity profile inside an organic solar cell a) with metallic Ag grating (period 700 nm) and b) with metallic grating plus Au NP (period 700 nm, particle size 15 nm).

In order to study the effect from the metallic nanoparticles in more details, Figure 7a shows the absorption enhancement from incorporation of different sizes of Au nanoparticles (15 nm, 35 nm, 55 nm), keeping a constant grating period of 700 nm in the device. Furthermore, the effect from the period of the arranged nanoparticles on the absorption efficiency is shown in Figure 7b, keeping the particle size constant at 15 nm.

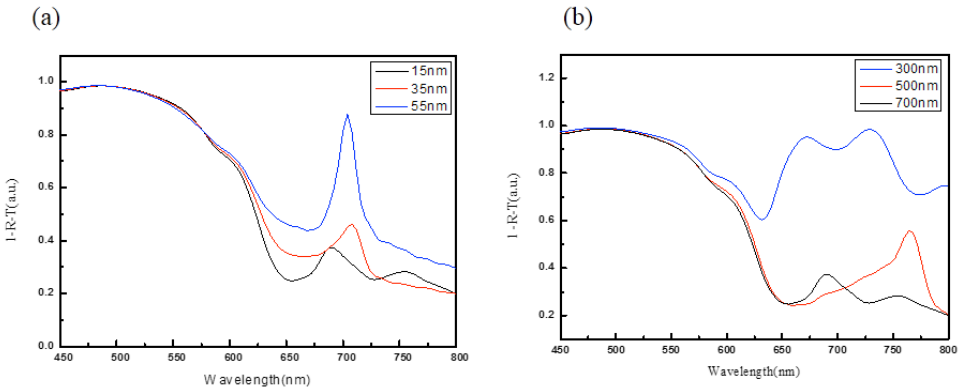

Figure 7. OSC stack absorption introducing the periodical nanoparticle and grating structure arrangement a) with a period of 700 nm, varying the Au particle size and b) with a particle size of 15 nm and varying the nanostructure period. By increasing the size of the particle (55 nm), keeping the same period, the absorption spectrum of the device enhances in the range from 600 nm up to 800 nm (figure 8a). By introducing 300 nm period grating, the absorption enhances significantly in the range of 640 nm up to 800 nm (figure 8b).

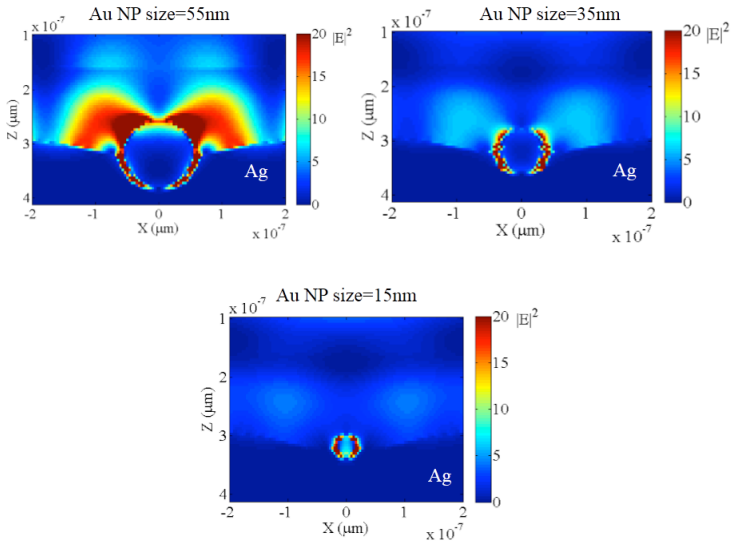

Figure 8. Electric field intensity profile for different Au NP sizes is plotted at 700nm excitation wavelength. The electric field intensity is increased significantly surrounding the nanoparticle and on the active layer by increasing the diameter of the Au nanoparticle.

For the different nanoparticle sizes, the electric field intensity profiles are also plotted for 700 nm excitation wavelength in Figure 9. Clearly, the results show that stronger light absorption enhancements in the organic layer are observed for nanoparticle sizes of about 55 nm in diameter. In general, increasing particle size leads to an increase of the integrated scattering intensity, which therefore enhances the optical path length of the incident photon within the device [8]. The strong near field enhancement can be explained by LPR due to Au NPs embedded at the interface between the active layer and HTL, as shown in Figure 8. The magnitude and the position of the near field resonances are strongly dependent on the type of the metal and of the size and shape of the particles [8]. By increasing the size of the nanoparticles, the strength of the near field and thus the absorption enhancement in the OSC increases. Figure 9c also demonstrates that the enhancement at 700nm for a 15 nm nanoparticle is stronger than at 600nm (figure 7b), explaining also the improved absorption observed at 650-800 nm in figure 6.

In addition, we studied the effect of the period of the arranged nanoparticles on the absorption efficiency. We considered the fixed value for the particle size (15 nm) and different periodic distances of 300 nm, 500 nm and 700 nm. For 1D periodic nanoparticle lines, two parameters become very important as the pattern does not have rotational symmetry: The inter particle distance, which we consider to be constant at 2 nm, and the period of the nanostructures [8]. Figure 7b shows that stronger absorption can be achieved for nanostructures with a period of 300 nm. The absorption enhancement in the region of 600 nm to 800 nm are ascribed to LPR hybridized with the different Floquet modes of the Ag nanostructure [26]. As shown in Figure 7 the broadband absorption enhancement is therefore achieved by introducing LPR of Au NPs and diffraction from the grating structure.

Although we find both experimentally and theoretically absorption enhancements in the investigated system, which can be explained by the combined diffraction effect and LPR of the nanoparticles, we observe experimentally that the nanoparticles only have a small effect in the range between 650-800 nm, where the enhancement should be strongest according to the numerical investigations. One explanation to these deviations could be the small variations in the imprinted grating structure (shape and size) and size distribution of the nanoparticles compared to the theoretical model.

5. CONCLUSIONS

In conclusion, periodically arranged gold nanoparticles have been demonstrated in single OSC units by means of a novel lithography-free nanoimprint method. We employ both scattering effects and localized surface plasmon resonances in order to achieve a broadband absorption enhancement. Numerical studies confirm the absorption enhancement observed experimentally, showing absorption enhancement and strong field enhancement surrounding the Au NPs by incorporating them into OSC devices. This technique opens up new pathways towards device applications, including efficient and cost-effective up-scaling.

Methods

Device fabrication: The device is realized on glass substrates coated with indium tin oxide (ITO), purchased from Lumtec (sheet resistance 9-15Ω/sq.), cleaned in ultrasonic bath with acetone and Isopropanol (10min each step). The substrate is covered with poly [(9,9-bis (3′-(N, N -dimethylamino) propyl)-2,7-fluorene)- alt -2,7-(9,9–dioctylfluorene)] (PFN) via spin-coating at 4000 rpm for 45 s. The PFN (1-materials) layer was dissolved in methanol in present of small amount of acetic acid (2μl ml^{-1}) [17]. Subsequently, the blend of the poly-3-hexylthiophene: [6,6]-phenyl-C61-butyric acid methyl ester (P3HT: PCBM) (1:1,weight ratio) ([2], purchased from Rieke Metals: Solenne) dissolved in chlorobenzene to form the active layer by spin-coating at 1500rpm for 45 s. In parallel, highly concentrated polyethylene glycol (PEG)-capped Au nanoparticles (4.07×10^{-7} M) suspended in ethanol were used for drop casting on to poly (dimethylsiloxane) (PDMS) wrinkled templates of 684± 20 nm pitch distances and 100±3.2 nm height for directed colloidal assembly of one-dimensional Au nanoscale lines. The soft-imprint process was carried out by applying a 500g weight on the backside of the PDMS templates while pressing against the ITO substrate covered with PFN and active layer. After the PDMS mold had been placed on the active layer, the whole sample was annealed on the hot plate at 140°C for 5 minutes. After removal of the PDMS mold, 10 nm of (molybdenum oxide) MoO_x and 100 nm of silver (Ag) thermally evaporated on the active layer with the periodical chain of nanoparticle at a pressure of $5*10^{-7}$ Torr.

Template fabrication: The PDMS slabs were prepared by mixing the cure agent and base monomer (Sylgard 184, Dow corning) at a 1:10 mass ratio. The mixture was cast onto Si wafers for ensuring a very low surface roughness and then let to outgas for 30 min followed by complete curing at 90^{o}C for 2 hours. The wrinkled poly (dimethylsiloxane) (PDMS) stamps were fabricated by pre-stretching 2 cm x 3 cm slabs using a made in-house clamp prior to air plasma treatment of the surface using a commercial plasma asher (Herrick PDC-a32G-2). By stretching the PDMS slabs in different amplitudes and by varying the oxygen plasma dose (d=power*time) onto the surface, one can tune the amplitude and period of a sinusoidal glass-like layer, which is formed from the buckling effect while the PDMS template is relaxed, due to a difference on the young module's of the glass-like surface to the bulk of the sample. This causes very well defined wrinkles on the surface of the elastomer [28]. The samples were stretched by ε=20%, the plasma cleaning power has been kept at 30W and the expose time was set to 5 min, 10 min and 25 min.

Gold nanoparticle fabrication: Citrate-stabilised spherical gold nanoparticles (NPs, diameter approximately 15 nm) were synthesized following a modified Turkevich-Frens method [29, 30]. 15.3 ml of a hot 40 mM trisodium citrate dehydrate solution was added to, $HAuCl_4$ trihydrate (0.2 mmol) in Milli-Q water (150 ml), which was already refluxing under vigorous stirring, and the whole mixture refluxed for a further 30 minutes. The solution was then cooled overnight under stirring and filtered through Whatman filter paper (grade 1 – 11 um pores) the next day. The particles where then subsequently stabilised by PEG which were prepared as follows: 0.47mM of PEG-OH was added to the solution and left overnight; this corresponds to approximately 10 times excess the estimated number of surface gold atoms on the NPs. The excess ligand was then removed by three cycles of centrifugations (15,000 rpm, 30 mins, 4^{o}C) and each time resuspended in 100% Ethanol. All nanoparticle solutions were characterized by UV/Vis spectroscopy to determine their concentration and approximate size [31]. Also the shift in the plasmon band was used to confirm ligand exchange had occurred.

Spectra were recorded in the range 400-800 nm using a Genesys 10S UV-Vis spectrophotometer (Thermo Scientific) and a 1 cm path length plastic disposable cuvette (Sarstedt, Germany).

Nanoimprint and optical characterization: Scanning electron microscope (Hitachi-S4800) was used to evaluate the assembly process on the PDMS samples and the imprint process itself. Total (specular plus diffuse) optical transmittance and reflectance were recorded using an UV-VIS-NIR Lambda 900 Perkin Elmer spectrophotometer, which is equipped with an integrating sphere (LabSphere).

Acknowledgments

This project has received funding from the European Union Seventh Framework Programme under grant agreement n° 607232 [THINFACE]. The work is performed within the PCAM European doctorate. A.L.F.C thanks the Brazilian CNPq Research council for providing a PhD scholarship under process number 213909/2012-0. C. K.-O. and A. M. D. thank the ERC Advanced Grant "PANDORA" under grant number 108269 for partial financial funding. The research leading to these results has received funding from the Innovation Fund Denmark under the project "SunTune".

References

[1] Shaw, P. E., Ruseckas, A., and Samuel, I. D. W., "Exciton Diffusion Measurements in Poly(3-hexylthiophene)," Advanced Materials, 20(18), 3516-3520 (2008).

[2] Hansen, R., Liu, Y., Madsen, M., and Rubahn, H., "Flexible organic solar cells including efficiency enhancing grating structures," Nanotechnology, 24(14), 145301 (2013).

[3] Li, X. H., Sha, W. E. I., Choy, W. C. H., Fung, D. D. S., and Xie, F. X., "Efficient inverted polymer solar cells with directly patterned active layer and silver back grating," Journal of Physical Chemistry C, 116, 7200-7206 (2012).

[4] Goszczak, A. J., Adam, J., Cielecki, P. P., Fiutowski, J., Rubahn, H.-G., and Madsen, M., "Nanoscale aluminum concaves for light-trapping in organic thin-films," Optics Communications, 370, 135-139 (2016).

[5] Park, H. I., Lee, S., Lee, J. M., Nam, S. A., Jeon, T., Han, S. W., and Kim, S. O., "High Performance Organic Photovoltaics with Plasmonic-Coupled Metal Nanoparticle Clusters," ACS Nano, 8(10), 10305-10312 (2014).

[6] Li, X., Choy, W. C. H., Lu, H., Sha, W. E. I., and Ho, A. H. P., "Efficiency Enhancement of Organic Solar Cells by Using Shape-Dependent Broadband Plasmonic Absorption in Metallic Nanoparticles," Advanced Functional Materials, 23(21), 2728-2735 (2013).

[7] Choy, W. C. H., and Ren, X., "Plasmon-Electrical Effects on Organic Solar Cells by Incorporation of Metal Nanostructures," IEEE Journal of Selected Topics in Quantum Electronics, 22, 1-9 (2016).

[8] Karg, M., König, T. A. F., Retsch, M., Stelling, C., Reichstein, P. M., Honold, T., Thelakkat, M., and Fery, A., "Colloidal self-assembly concepts for light management in photovoltaics," Materials Today, 18(4), 185-205 (2015).

[9] Lu, L., Luo, Z., Xu, T., and Yu, L., "Cooperative plasmonic effect of Ag and Au nanoparticles on enhancing performance of polymer solar cells," Nano Letters, 13, 59-64 (2013).

[10] Fu, W.-F., Chen, X., Yang, X., Wang, L., Shi, Y., Shi, M., Li, H.-Y., Jen, A. K.-Y., Chen, J.-W., Cao, Y., and Chen, H.-Z., "Optical and electrical effects of plasmonic nanoparticles in high-efficiency hybrid solar cells.," Physical chemistry chemical physics : PCCP, 15, 17105-11 (2013).

[11] Choi, H., Lee, J.-p., Ko, S.-j., Jung, J.-w., Park, H., Yoo, S., Park, O., Jeong, J.-r., Park, S., and Kim, J. Y., "Multipositional Silica-Coated Silver Nanoparticles for High- Performance Polymer Solar Cells," (2013).

[12] Baek, S. W., Park, G., Noh, J., Cho, C., Lee, C. H., Seo, M. K., Song, H., and Lee, J. Y., "Au@Ag core-shell nanocubes for efficient plasmonic light scattering effect in low bandgap organic solar cells," ACS Nano, 8, 3302-3312 (2014).

[13] Yao, K., Salvador, M., Chueh, C.-C., Xin, X.-K., Xu, Y.-X., DeQuilettes, D. W., Hu, T., Chen, Y., Ginger, D. S., and Jen, A. K.-Y., "A General Route to Enhance Polymer Solar Cell Performance using Plasmonic Nanoprisms," Advanced Energy Materials, n/a-n/a (2014).

[14] Baek, S.-W., Noh, J., Lee, C.-H., Kim, B., Seo, M.-K., and Lee, J.-Y., "Plasmonic forward scattering effect in organic solar cells: a powerful optical engineering method.," Scientific reports, 3, 1726 (2013).

[15] Zampetti, A., Fallahpour, A. H., Dianetti, M., Salamandra, L., Santoni, F., Gagliardi, A., Auf der Maur, M., Brunetti, F., Reale, A., Brown, T. M., and Di Carlo, A., "Influence of the interface material layers and

semiconductor energetic disorder on the open circuit voltage in polymer solar cells," Journal of Polymer Science Part B: Polymer Physics, 53(10), 690-699 (2015).
[16] Fallahpour, A. H., Ulisse, G., Auf der Maur, M., Di Carlo, A., and Brunetti, F., "3-D Simulation and Optimization of Organic Solar Cell With Periodic Back Contact Grating Electrode," Photovoltaics, IEEE Journal of, 5(2), 591-596 (2015).
[17] He, Z., Zhong, C., Su, S., Xu, M., Wu, H., and Cao, Y., "Enhanced power-conversion efficiency in polymer solar cells using an inverted device structure," Nat Photon, 6(9), 591-595 (2012).
[18] Monestier, F., Simon, J.-J., Torchio, P., Escoubas, L., Flory, F., Bailly, S., de Bettignies, R., Guillerez, S., and Defranoux, C., "Modeling the short-circuit current density of polymer solar cells based on P3HT:PCBM blend," Solar Energy Materials and Solar Cells, 91(5), 405-410 (2007).
[19] Tumbleston, J. R., Ko, D. H., Samulski, E. T., and Lopez, R., "Absorption and quasiguided mode analysis of organic solar cells with photonic crystal photoactive layers," Opt Express, 17(9), 7670-81 (2009).
[20] Palik, E. D., [Handbook of Optical Constants of Solids] Academic Press, (1998).
[21] Fallahpour, A. H., Gentilini, D., Gagliardi, A., Maur, M. A. d., Lugli, P., and Carlo, A. d., "Systematic Study of the PCE and Device Operation of Organic Tandem Solar Cells," IEEE Journal of Photovoltaics, 6(1), 202-210 (2016).
[22] Burkhard, G. F., Hoke, E. T., and McGehee, M. D., "Accounting for interference, scattering, and electrode absorption to make accurate internal quantum efficiency measurements in organic and other thin solar cells," Advanced Materials, 22(30), 3293-3297 (2010).
[23] Peumans, P., Yakimov, A., and Forrest, S. R., "Small molecular weight organic thin-film photodetectors and solar cells," Journal of Applied Physics, 93(7), 3693-3723 (2003).
[24] Fallahpour, A. H., Gagliardi, A., Gentilini, D., Zampetti, A., Santoni, F., Auf der Maur, M., and Di Carlo, A., "Optoelectronic simulation and thickness optimization of energetically disordered organic solar cells," Journal of Computational Electronics, 13(4), 933-942 (2014).
[25] Fallahpour, A. H., Gagliardi, A., Santoni, F., Gentilini, D., Zampetti, A., Auf der Maur, M., and Di Carlo, A., "Modeling and simulation of energetically disordered organic solar cells," Journal of Applied Physics, 116(18), 184502 (2014).
[26] Li, X., Choy, W. C. H., Huo, L., Xie, F., Sha, W. E. I., Ding, B., Guo, X., Li, Y., Hou, J., You, J., and Yang, Y., "Dual plasmonic nanostructures for high performance inverted organic solar cells," Advanced Materials, 24, 3046-3052 (2012).
[27] Niesen, B., Rand, B. P., Van Dorpe, P., Cheyns, D., Tong, L., Dmitriev, A., and Heremans, P., "Plasmonic Efficiency Enhancement of High Performance Organic Solar Cells with a Nanostructured Rear Electrode," Advanced Energy Materials, 3(2), 145-150 (2013).
[28] Schweikart, A., Horn, A., Böker, A., and Fery, A., "Controlled wrinkling as a novel method for the fabrication of patterned surfaces," Advances in Polymer Science, 227, 75-99 (2010).
[29] Turkevich, J., Stevenson, P. C., and Hillier, J., "A study of the nucleation and growth processes in the synthesis of colloidal gold," Discussions of the Faraday Society, 11(0), 55 (1951).
[30] Frens, G., "Controlled Nucleation for regulation of Particle-Size in Monodisperse Gold Suspensions.," Nature,Phys.Sci, 241, 20-22 (1973).
[31] Haiss, W., Thanh, N. T., Aveyard, J., and Fernig, D. G., "Determination of size and concentration of gold nanoparticles from UV-vis spectra," Anal Chem, 79(11), 4215-21 (2007).